ELSEVIER

Journal of Biomechanics 37 (2004) 27–35

JOURNAL OF BIOMECHANICS

www.elsevier.com/locate/jbiomech
www.JBiomech.com

Comparison of the elastic and yield properties of human femoral trabecular and cortical bone tissue

Harun H. Bayraktar[a,*], Elise F. Morgan[a], Glen L. Niebur[b], Grayson E. Morris[a], Eric K. Wong[a], Tony M. Keaveny[a,c]

[a] *Orthopaedic Biomechanics Laboratory, Department of Mechanical Engineering, University of California, 2166 Etcheverry Hall, Berkeley, CA 94720-1740, USA*

[b] *Department of Aerospace and Mechanical Engineering, University of Notre Dame, 376 Fitzpatrick Hall, Notre Dame, IN 46556, USA*

[c] *Department of Bioengineering, University of California, 6175 Etcheverry Hall, Berkeley, CA 94720-1740, USA*

Accepted 23 June 2003

Abstract

The ability to determine trabecular bone tissue elastic and failure properties has biological and clinical importance. To date, trabecular tissue yield strains remain unknown due to experimental difficulties, and elastic moduli studies have reported controversial results. We hypothesized that the elastic and tensile and compressive yield properties of trabecular tissue are similar to those of cortical tissue. Effective tissue modulus and yield strains were calibrated for cadaveric human femoral neck specimens taken from 11 donors, using a combination of apparent-level mechanical testing and specimen-specific, high-resolution, nonlinear finite element modeling. The trabecular tissue properties were then compared to measured elastic modulus and tensile yield strain of human femoral diaphyseal cortical bone specimens obtained from a similar cohort of 34 donors. Cortical tissue properties were obtained by statistically eliminating the effects of vascular porosity. Results indicated that mean elastic modulus was 10% lower ($p<0.05$) for the trabecular tissue (18.0 ± 2.8 GPa) than for the cortical tissue (19.9 ± 1.8 GPa), and the 0.2% offset tensile yield strain was 15% lower for the trabecular tissue (0.62 ± 0.04% vs. 0.73 ± 0.05%, $p<0.001$). The tensile–compressive yield strength asymmetry for the trabecular tissue, 0.62 on average, was similar to values reported in the literature for cortical bone. We conclude that while the elastic modulus and yield strains for trabecular tissue are just slightly lower than those of cortical tissue, because of the cumulative effect of these differences, tissue strength is about 25% greater for cortical bone.

Keywords: Cancellous bone; Finite element modeling; Bone strength; Yield strain; Elastic modulus

1. Introduction

The mechanical properties of trabecular bone depend on volume fraction, architecture, and trabecular tissue material properties. Characterization of the latter and its role in trabecular bone mechanical behavior has potential clinical and biological importance. Clinically, knowledge of the elastic and failure properties of trabecular tissue could be used to investigate the effects of drug treatments, aging, and disease at the tissue level. Biologically, these properties, and their relation to cortical tissue properties, could provide insight into general structure-function relationships for bone. Tissue-level elastic and yield properties are also required as input for both computational (Niebur et al., 2000; Silva and Gibson, 1997; van Rietbergen et al., 1995; Yeh and Keaveny, 1999) and analytical (Gibson, 1985) models, and therefore represent an important basis for micromechanical analysis of trabecular bone.

Although the tissue-level elastic properties of trabecular bone have been reported in numerous studies (Table 1; also see Guo, 2001 for a more detailed review), because of technical challenges, there remain substantial discrepancies in these data and there are almost no data available for tissue-level failure properties. An alternative approach to direct mechanical testing at the tissue level is to use high-resolution finite element models,

*Corresponding author. Tel.: +1-510-642-3787; fax: +1-510-642-6163.

E-mail addresses: harun@me.berkeley.edu (H.H. Bayraktar), tmk@me.berkeley.edu (T.M. Keaveny).

0021-9290/$ - see front matter © 2003 Elsevier Ltd. All rights reserved.
doi:10.1016/S0021-9290(03)00257-4

Table 1
A comparison of elastic moduli of trabecular tissue, E_{tissue} (mean ± SD, in GPa), reported in the literature and in the current study

Reference	Anatomic site	Method	Spec./indent.[a] (donors)	E_{tissue} (GPa)
Ulrich et al. (1997)	Human femoral head	Experiment-FEA	6 (6)	3.5–8.6[b]
Rho et al. (1997)	Human vertebra	Nanoindentation[c]	72 (2)	13.4 ± 2.0
Hou et al. (1998)	Human vertebra	Experiment-FEA	28 (28)	5.7 ± 1.6
Ladd et al. (1998)	Human vertebra	Experiment-FEA	5 (5)	6.6 ± 1.0
Turner et al. (1999)	Human distal femur	Nanoindentation[c]	30 (1)	18.1 ± 1.7
		Acoustic microscopy	3 (1)	17.5 ± 1.1
Zysset et al. (1999)	Human femoral neck	Nanoindentation	N/A[d] (8)	11.4 ± 5.6
Niebur et al. (2000)	Bovine proximal tibia	Experiment-FEA[e]	7 (7)	18.7 ± 3.4
This study	Human femoral neck	Experiment-FEA[e]	12 (11)	18.0 ± 2.8

See Guo (2001) for a more comprehensive review, which includes cortical bone.
[a] Number of specimens (or indentations for nanoindentation studies) and donors used in the study.
[b] Only range reported.
[c] Specimens were dehydrated.
[d] Information not available.
[e] Endcaps were used to eliminate end artifacts in the apparent-level mechanical testing.

derived from micro-computed tomography (micro-CT) scans, together with specimen-specific experimental data at the whole specimen (apparent) level to calibrate "effective" elastic properties of the tissue (van Rietbergen et al., 1995). Most of these types of studies have used compression testing with platens to provide the calibration data. However, because of the associated end-artifacts (Jacobs et al., 1999; Keaveny et al., 1997; Odgaard and Linde, 1991), such studies have reported low values of calibrated effective tissue moduli (Hou et al., 1998; Ladd et al., 1998) when compared to the experimental studies (Rho et al., 1997; Turner et al., 1999; Zysset et al., 1999) that used ultrasound and nanoindentation or the finite element-experimental studies (Niebur et al., 2000) that used testing protocols that minimized end-artifacts at the apparent level. Regarding failure properties, by using a combination of nonlinear, high-resolution finite element analyses and apparent-level mechanical tests (Niebur et al., 2000), it was found that the tissue-level tension-compression strength asymmetry for bovine trabecular bone was close to values reported for bovine cortical bone (Burstein et al., 1976; Reilly and Burstein, 1975). However, except for the fatigue strength of micro-beam specimens (Choi and Goldstein, 1992), no studies have reported failure properties for human trabecular tissue.

In any study comparing trabecular tissue mechanical properties to those of cortical tissue, porosity, orientation, anatomic site, degree of mineralization, and age need to be controlled. Focusing on a cohort of specimens from elderly human femora, addressing longitudinal behavior, and accounting for vascular porosity effects, our goal was to test the hypothesis that trabecular and cortical tissue have similar elastic and yield properties. Using an approach that included high-resolution finite element analysis and various types of mechanical testing, our specific objectives were to: (1) determine the effective tissue-level elastic modulus and tissue tensile and compressive yield strains for human femoral neck trabecular bone; and (2) compare these properties with cortical tissue elastic and yield properties obtained from tension testing, using tissue from a similar cohort of donors. While this study is complementary to others on tissue-level elastic properties (Rho et al., 1999; Turner et al., 1999; Zysset et al., 1999), it is novel in its focus on yield behavior.

2. Materials and methods

2.1. Trabecular bone

Twelve human trabecular bone specimens from 11 cadavers (six male, five female; mean age 65.5 ± 9.1 yr, age range 51–85) were studied. The two specimens obtained from the same donor were taken from similar locations in the right and left femoral neck. Eight-millimeter diameter, 32-mm long (nominally) specimens were extracted from the femoral neck, aligned with their principal trabecular orientation as determined by contact radiographs (Keaveny et al., 1994; Morgan and Keaveny, 2001). Specimens were kept hydrated at all times, wrapped in plastic, and stored at –20°C in air tight containers until mechanical testing. Uniaxial mechanical testing was conducted at room temperature. Six specimens were mechanically tested in tension using endcaps and six were tested under compression using platens with an extensometer attached to the side of the specimen to minimize end-artifacts (see Morgan and Keaveny, 2001 for details on the experimental protocols). Specimens were tested at a strain rate of 0.5%/s just to the 0.2% offset yield point (which preserves the trabecular architecture intact), and apparent elastic

modulus, apparent yield strain and yield stresses were recorded.

After testing, the specimens were cleaned of marrow and excess water, and volume fractions were measured using Archimedes' principle. Apparent density was calculated as the hydrated mass divided by the bulk volume. The mean (±S.D.) volume fraction of the 12 specimens was 0.29±0.05, ranging from 0.20 to 0.36. Apparent density of the 12 trabecular bone specimens ranged from 0.43 to 0.75 g/cm^3 with a mean 0.62±0.09 g/cm^3. High-resolution images were then obtained using either CNC serial milling (Beck et al., 1997) or micro-CT (Scanco Medical AG, Bassersdorf, Switzerland) at 10 and 22 μm resolutions, respectively. To decrease computation time, region averaging was used to scale all image resolutions to (mean±S.D.= 63±5 μm, range 52–66 μm) less than one-fourth of the mean trabecular thickness (mean±S.D.=294.6± 48.0 μm) for all specimens, as recommended for numerical convergence (Guldberg et al., 1998; Niebur et al., 1999). The numerical error introduced in the apparent-level modulus, compared to a 20 μm element size model was approximately 7% (Niebur et al., 1999). The mass-compensated thresholding technique (Ulrich et al., 1998) was used to threshold the gray-scale images.

The first step in the overall stress analysis was to determine the effective tissue-level modulus for each specimen. A cylindrical high-resolution finite element model was created for each specimen by converting each bone voxel into an eight-node finite element (Hollister et al., 1994). The cylindrical models had a nominal diameter of 8 mm and lengths ranging from 8 to 16 mm, which was the specimen length between the endcaps. The models contained from 393,300 to 1,064,382 elements. Using a custom finite element code, a single step linear analysis was performed to determine the ratio of effective tissue modulus to apparent modulus for each model. This ratio was then multiplied by the experimentally measured apparent modulus on a per specimen basis to determine the specimen-specific effective tissue-level modulus, E_{tissue} (van Rietbergen et al., 1995).

The second step was to determine the tissue tensile and compressive yield properties by performing a series of nonlinear analyses. Finite element models having from 107,538 to 187,394 elements, depending on volume fraction, were created from a 5 mm cube region near the center of each cylinder. These smaller models, as opposed to the larger cylindrical models, were used to reduce computational costs. To justify this strategy, nonlinear analyses of tensile and compressive loading were performed for three specimens with volume fractions 20%, 27% and 36%, for both the 5 mm cube and the cylinder models. While apparent modulus of the 5 mm cubes differed as much as 9.5% from that of the cylinder due to localized volume fraction variations, the percentage differences in predicted apparent yield strains ranged from only 0.4% to 3.2%, whereas the savings in computational costs was over five-fold.

For all nonlinear analyses, trabecular tissue was modeled as a bilinear elastic material using a tensile–compressive asymmetric principal strain failure criterion (Fig. 1) (Niebur et al., 2000). The specimen-specific initial value of E_{tissue} previously determined from the linear analyses was used in each model. After reaching the yield point, post-yield modulus was set to 5% of E_{tissue} (Fig. 1). This reduction was based on our post-yield modulus measurement of cortical bone specimens (94.2%) and a previously reported value, 95.4%, for cortical bone (Reilly and Burstein, 1975). Since the post-yield modulus of trabecular tissue is not known, the sensitivity of the results to the post-yield modulus was investigated, in order to justify this assumption. By independently varying this post-yield modulus between 1% and 9% of E_{tissue} in both tension and compression, percent differences of less than 6% were observed in predictions of both apparent-level tensile and compressive yield strains. When the tensile post-yield modulus was kept constant at 5% of E_{tissue}, varying the compressive post-yield modulus alone from 1% to 9% of E_{tissue} changed the predicted apparent compressive yield strain by less than 1.6%.

In order to design the calibration procedure for the tissue yield strain, the sensitivity of apparent-level yield strains to tissue-level tensile and compressive yield strains was investigated. Apparent-level tensile yield strains were largely independent of the tissue-level compressive yield strain, consistent with behavior reported previously for bovine bone (Niebur et al., 2000). This trend enabled us to calibrate the tissue

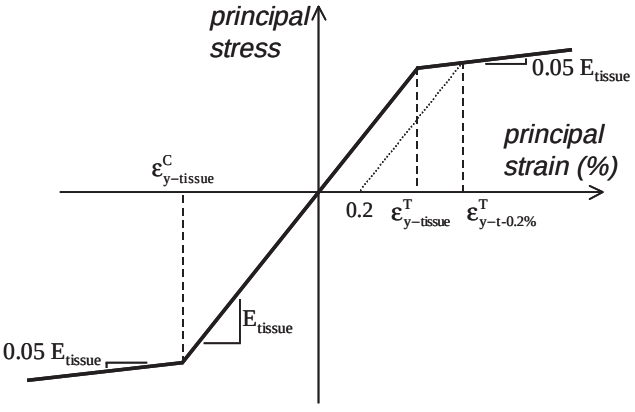

Fig. 1. Bilinear tissue-level constitutive model (not to scale, adapted from Niebur et al., 2000). The post-yield modulus was set to 5% of the initial modulus when the principal strains exceeded either the tensile ($\varepsilon^T_{y\text{-}tissue}$) or compressive ($\varepsilon^C_{y\text{-}tissue}$) tissue yield strains. To provide a basis for comparison with cortical bone, 0.2% offset yield strains and stresses were also calculated for this material model. While unloading was assumed to follow the same path as loading, it was confirmed that less than 0.05% of the elements experienced any unloading during monotonic tensile or compressive loading.

tensile yield strain independently of the tissue compressive yield strain using the algorithm shown in Fig. 2. Initial estimates of tissue tensile ($\varepsilon^{T}_{y\text{-tissue}}$) and compressive ($\varepsilon^{C}_{y\text{-tissue}}$) yield strains, based on bovine data (Niebur et al., 2000), were used in a nonlinear analysis. The resulting apparent tensile yield strain ($\varepsilon^{T}_{y\text{-tissue}}$) was compared to the specimen-specific experimental value. If the percentage difference was less than or equal to 0.1%, the loop was terminated; if not, a new estimate of $\varepsilon^{T}_{y\text{-tissue}}$ was obtained by linear scaling and iterations were continued until convergence. During this calibration, $\varepsilon^{C}_{y\text{-tissue}}$ was held constant. After all six tensile specimens were calibrated, the mean tissue effective tensile yield strain $\bar{\varepsilon}^{T}_{y\text{-tissue}}$ was then used in a similar calibration scheme for the tissue compressive yield strain. In this way, the effective tissue yield strain in compression $\varepsilon^{C}_{y\text{-tissue}}$ was calibrated for six additional specimens. Tissue yield strains were calibrated using at most three iterations for each of the 12 specimens.

For the nonlinear analyses, apparent-level loads were applied quasi-statically using an implicit incremental algorithm. The resulting nonlinear system of equations was solved at each increment using the Newton-Raphson method. An element-by-element preconditioned conjugate gradient solver (Hughes et al., 1987) was used to solve the linear system of equations at each increment. All models were analyzed on either a Cray T3E (Cray Inc., Seattle, WA) or IBM SP2 (IBM Corp., Armonk, NY) distributed memory parallel supercomputer. The linear and nonlinear analyses on average required 21 and 236 CPU hours, respectively, per specimen. In total, 10,675 CPU hours were used.

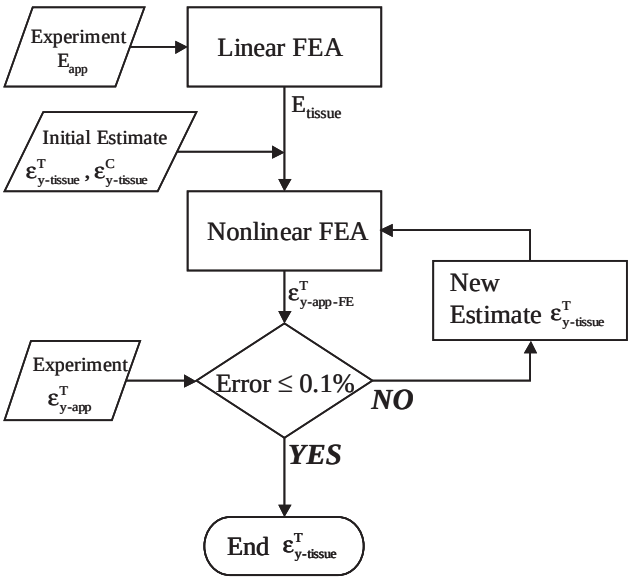

Fig. 2. Flowchart for tissue effective property calibration. First, the tissue effective modulus was calibrated using experimental data (E_{app}). Then a nonlinear finite element analysis (FEA) was run using initial estimates for tissue yield strains, $\varepsilon^{T}_{y\text{-tissue}}$ and $\varepsilon^{C}_{y\text{-tissue}}$ (the latter held constant during $\varepsilon^{T}_{y\text{-tissue}}$ calibration). The resulting apparent yield strain ($\varepsilon^{T}_{y\text{-app-FE}}$) was compared to the experimental value ($\varepsilon^{T}_{y\text{-app}}$) to check if the percent difference was less than 0.1%. If not, a new estimate for $\varepsilon^{T}_{y\text{-tissue}}$ was obtained and the process was repeated until convergence.

2.2. Cortical bone

Seventy-four reduced-section cortical bone specimens ($2.5 \times 3.0 \times 11\,mm^3$ gage section) from 34 cadavers (22 male; 12 female, mean age 71.8 ± 8.8 yr, range 54–85) were excised longitudinally from the cortical wall at the mid-diaphyseal region of femur. While the mean age of the cortical bone donors was 6.3 yr greater than ($p < 0.045$) for the trabecular bone donors, the age range was similar, and four of the cortical bone donors were also the origin of our trabecular bone specimens.

Mechanical testing was performed in uniaxial tension using a servo-hydraulic load frame (Mini-bionics 858, MTS Corp., Eden Prairie, MN) in displacement control at a strain rate of 0.2%/s. Specimens were attached to the load frame using a three-jawed chuck and then lowered into uncured polymethylmethacrylate (PMMA) which then set, in order to eliminate gripping-induced bending. All specimens were wrapped in saline-soaked gauze throughout the process to prevent their dehydration. Strain was measured using a 5 mm extensometer (Model #632.29F-30, MTS Corp., Eden Prairie, MN) attached within the gage length of the specimens. Elastic modulus, 0.2% offset yield stresses and strains, and post-yield modulus were recorded.

After testing, three thin transverse sections ($\sim 200\,\mu m$) were cut from the gage length close to the fracture site using a precision diamond saw (Isomet 1000, Buehler Ltd., Lake Bluff, IL). A digital image of each slice at 2.15 μm resolution was captured (AxioCam, Carl Zeiss, Germany) and digitally thresholded using Adobe Photoshop (Adobe Inc., San Jose, CA) and NucMed Image (NIH, Rockville, MD). The number of pixels lying inside pores divided by the total number of pixels in the cross-section determined the vascular porosity. Since lacunae are also present in trabecular bone tissue they were excluded from the cortical bone porosity calculation. This was done by ignoring all pores having areas less than $175\,\mu m^2$. Cortical tissue elastic modulus and yield stresses for each specimen were calculated from the modulus-porosity linear regression obtained for all 74 specimens by using the regression to extrapolate modulus values to zero vascular porosity. In this way, we distinguish cortical bone from cortical tissue; the former referring to bone that includes vascular porosity, the latter excluding such porosity. Yield strains did not depend on porosity and therefore no distinction was made between yield strains between cortical bone vs. tissue.

Trabecular and cortical tissue yield stresses and strains were compared using Student's *t*-test in Microsoft Excel

2000 (Microsoft Corp., Redmond, WA). Analysis of covariance was performed to compare the dependence of trabecular vs. cortical bone yield stress on elastic modulus (JMP 5.0, SAS Inst., Cary, NC).

3. Results

The mean (±S.D.) value of the effective trabecular tissue modulus calibrated for the 12 trabecular bone specimens was 18.0±2.8 GPa, ranging from 12.1 to 22.2 GPa. Linear regression analysis indicated that this parameter did not depend on the measured volume fraction ($p > 0.99$), apparent modulus ($p > 0.34$), or apparent density ($p > 0.94$, Fig. 3a).

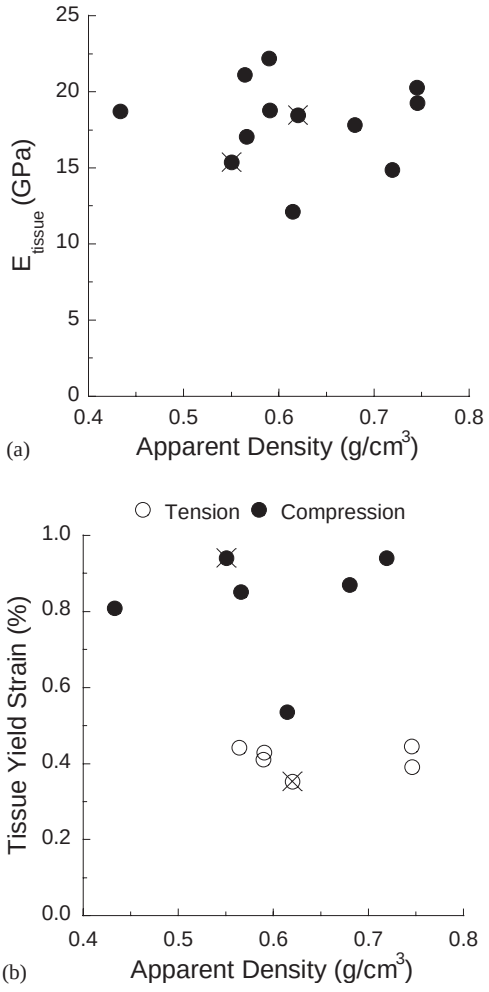

Fig. 3. (a) Calibrated effective tissue modulus did not depend on apparent density ($p > 0.94$). The coefficient of variation of tissue modulus was 15.7%; values ranged from 12.1 to 22.2 GPa. The two marked data points (×) are for the two specimens from the same donor, one tested in tension and the other in compression. (b) Calibrated tissue tensile and compressive yield strains were both independent of apparent density ($p > 0.81$). Tissue compressive yield strains were significantly higher than tissue tensile yield strains ($p < 0.001$).

The mean values (±S.D.) of the calibrated trabecular tissue tensile and compressive yield strains were 0.41±0.04% and 0.83±0.15%, respectively, and the difference was statistically significant ($p < 0.001$, Fig. 3b). The percent coefficient of variation (S.D./mean) in tissue tensile yield strain of only 8.6% was less than half the value for compression (18.3%). Similar to effective tissue modulus, both tissue-level tensile and compressive yield strains did not depend on apparent density ($p > 0.81$), volume fraction ($p > 0.97$), or apparent modulus ($p > 0.34$, Fig. 3b). The corresponding values of tissue yield stresses (product of tissue modulus and tissue yield strain) in tension and compression were 82.8±11.1 and 133.6±34.1 MPa, respectively. The tensile–compressive ratio of these values was 0.62 on average.

Mean (±S.D.) elastic modulus and post-yield modulus of cortical bone were 17.8±2.1 and 1.03±0.04 GPa, respectively. The mean porosity of

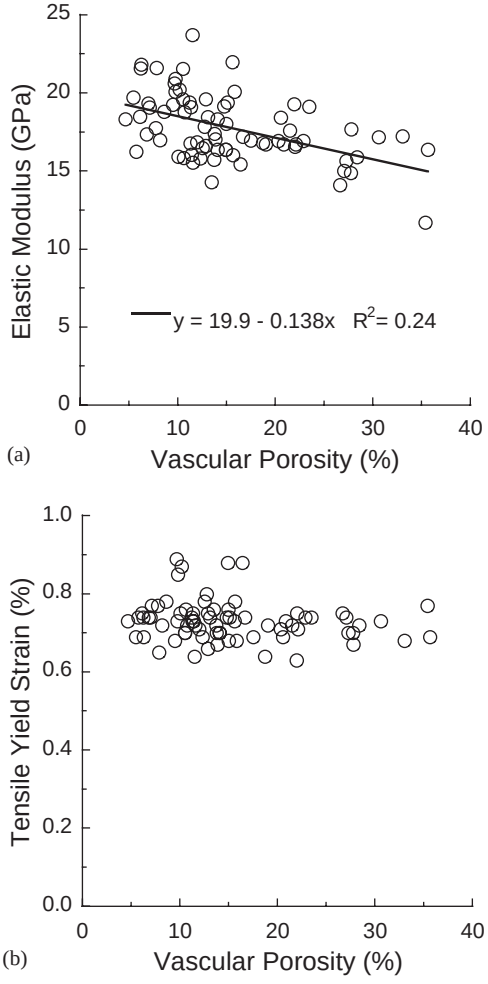

Fig. 4. (a) Cortical *bone* elastic modulus was negatively correlated with porosity ($p < 0.001$). Cortical *tissue* elastic modulus was calculated for each specimen by extrapolating measured value to a zero-porosity value using this regression. (b) Cortical bone 0.2% offset tensile yield strain showed no dependence on porosity ($p > 0.13$).

cortical bone specimens was 15.3±7.5%, ranging from 4.6% to 35.6%. While cortical bone elastic modulus and yield stresses (without subtracting out effects of porosity) were negatively correlated with porosity ($p<0.001$, Fig. 4a), the 0.2% offset yield strains exhibited no significant correlation ($p=0.136$, Fig. 4b). Therefore, cortical bone yield strains were used in the comparison between cortical tissue and trabecular tissue. After adjusting for zero-porosity, cortical tissue elastic modulus was on average 11% higher than that of the trabecular tissue (Table 2), and displayed a coefficient of variation of less than 12%. Yield strains and stresses were 17% and 27%, respectively, higher for cortical tissue than trabecular tissue (Fig. 5a, Table 2). These trends were also observed in the subset of data for the trabecular and cortical specimens originating from the same donors (Table 3). While no significant difference between cortical vs. trabecular tissue was found in the slope of the yield stress-tissue elastic modulus regressions ($p>0.437$), the elevation was greater for cortical tissue ($p<0.001$, Fig. 5b). This indicates that, for a given tissue modulus, cortical tissue is on average 20–30% stronger than trabecular tissue.

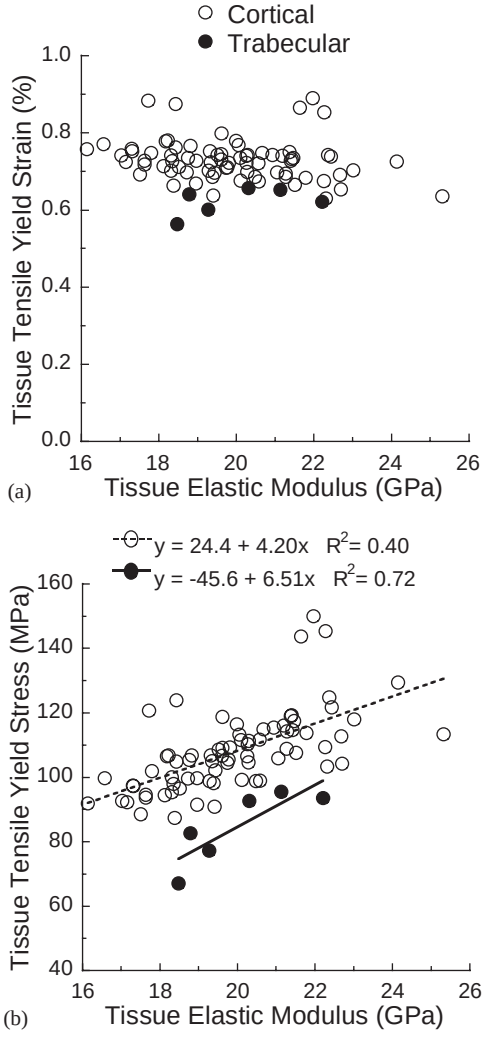

Fig. 5. (a) Cortical tissue 0.2% tensile yield strains were higher on average by 18% than trabecular tissue 0.2% tensile yield strains ($p<0.001$), but neither displayed any dependence on tissue elastic modulus ($p>0.07$); (b) 0.2% tensile yield stress-elastic modulus regressions indicate a difference in elevation ($p<0.001$) but not in the slope ($p>0.437$) between the trabecular and cortical tissue.

4. Discussion

Trabecular and cortical tissue properties are of great interest in the etiology of osteoporosis since it is widely speculated that this aspect of bone "quality" does affect fracture risk (Heaney, 1993). Considering that elastic and strength properties at the apparent (whole specimen) level for cortical vs. trabecular bone can vary by orders of magnitude, cortical tissue and trabecular tissue have remarkably similar elastic and (yield) strain properties. The tensile-compressive asymmetry in yield strength of trabecular tissue is also similar to that of cortical bone, based on literature reports of the latter: for human femoral cortical bone, the average ratio of tensile to compressive yield strength has been reported as 0.56 (Burstein et al., 1976; Reilly and Burstein, 1975), which is in close agreement with the value 0.62 obtained in our study for the trabecular tissue. However, there do appear to be subtle differences. Most notably, due to the cumulative effects of small differences in elastic modulus and yield strain between the two types of bone tissue, tissue strength for a given elastic modulus is higher by 20–30% for cortical bone.

The main novelty of this study was its focus on yield properties at the tissue level for both cortical and trabecular bone. For the latter, this was made possible by the use of nonlinear finite element analysis of trabecular bone specimens in conjunction with apparent level experimental data gathered from the same specimens and using techniques that eliminated end-artifacts (Keaveny et al., 1997; Morgan and Keaveny, 2001). We are aware of no other studies that have provided measures of yield properties for human trabecular tissue, although our values are similar to what we found for bovine trabecular tissue (Niebur et al., 2000) using a mostly similar technique to that used here. In this study, the trabecular bone was taken from 11 elderly donors spanning a large range of volume fractions (20–36%), whereas the cortical bone was taken from a similar but larger cohort that included four of the same donors. Our combined experimental-computational approach circumvented the substantial technical challenge of measurement of yield properties for trabecular tissue due to the small and irregular size of individual trabeculae, and produced "effective"—or volume-averaged—values of the tissue properties on a per-specimen basis. For cortical *tissue*, the zero-porosity mechanical properties

Table 2
Comparison of mean (±S.D.) values of elastic modulus and yield properties for trabecular tissue vs. cortical tissue

	Trabecular	Cortical[a]	p-Value[b]
Elastic modulus (GPa)	18.0±2.8 ($n=12$)	19.9±1.8 ($n=74$)	0.044
Tension			
0.2% offset yield strain (%)	0.62±0.04 ($n=6$)	0.73±0.05 ($n=74$)	<0.001
0.2% offset yield stress (MPa)	84.9±11.2 ($n=6$)	107.9±12.3 ($n=74$)	0.003
Compression			
0.2% offset yield strain (%)	1.04±0.15 ($n=6$)	N/A	N/A
0.2% offset yield stress (MPa)	135.3±34.3 ($n=6$)	N/A	N/A

N/A—No cortical bone compressive tests were performed.
[a] Cortical tissue elastic modulus and yield stresses for each specimen were calculated from the modulus-porosity regression (Fig. 4a) obtained for all 74 specimens, by extrapolating to values having zero vascular porosity.
[b] p-Values for Student's unpaired t-test with unequal variances comparing trabecular vs. cortical properties.

Table 3
Paired measurements of elastic modulus and tensile yield strain of trabecular tissue and cortical bone from the same donors

Donor			Elastic modulus (GPa)		Tensile yield strain[a] (%)		Tensile yield stress[a] (MPa)	
Age	Sex	Specimens[b]	Trabecular	Cortical	Trabecular	Cortical	Trabecular	Cortical
63	M	1	21.1	20.3	0.65	0.74	95.6	111.4
62	F	2	22.2	18.9	0.62	0.76	93.6	106.8
72	M	2	19.3	20.9	0.60	0.75	77.4	114.3
66	M	2	17.8	19.8	N/A[c]	0.71	N/A[c]	104.9

[a] 0.2% offset values.
[b] Number of cortical bone specimens for each donor. Cortical tissue elastic modulus and yield strain values reported are average values.
[c] This trabecular bone specimen was tested in compression and therefore a per specimen calibrated value of tensile tissue yield strain was not available.

represent the properties of cortical *bone* having no vascular porosity.

Despite the strengths of our study, certain limitations exist. First, two mostly distinct groups of donors were used for the trabecular and cortical bone specimens. However, due to the small average age difference (6 yr), the overlapping age range, the four common donors, and the large sample size for the cortical bone we believe any possible biases introduced by sampling effects are minor. Second, two different techniques were used to obtain mechanical properties of the two types of tissue. Due to the experimental difficulties involved in accurately testing single trabeculae, a surrogate experimental–computational technique was developed to allow comparison between the two types of tissue. An important assumption of high-resolution finite element studies is the assumed uniformity of tissue-level properties across all elements in the finite element model. It has been demonstrated using nanoindentation testing that the coefficient of variation in trabecular tissue modulus ranges from 22% to 63% across donors for the human femur (our calculations from the reported data) (Zysset et al., 1999). Parametric finite element analyses have shown that including intra-trabecular variations does reduce the predicted apparent modulus, and the effect depends primarily on the spatial distribution of modulus within the trabeculae (Jaasma et al., 2002; van der Linden et al., 2001). We estimate that the effective tissue modulus obtained from our analyses underestimate the actual mean tissue modulus value by approximately 10% (Jaasma et al., 2002), and the same may be true for the yield properties. Thus, the differences in properties reported here between the two types of tissues are best interpreted as upper bounds on any true differences.

The effective yield properties reported here are likely dominated by the material behavior of the trabecular tissue as opposed to any nonlinear kinematic effects. Our finite element modeling, which did not include any geometric nonlinearity (i.e. large deformations), may not be suitable to predict the micromechanical failure behavior of trabecular bone at low density sites such as the vertebra, tibia or greater trochanter, where large deformations may be important (Gibson, 1985; Müller et al., 1998). However, the advantage of analyzing femoral neck trabecular bone, as we did here, is that such geometric effects are expected to be minimal due to the high-density nature of this type of trabecular bone—the strongest reported in the human body (Morgan and Keaveny, 2001). Since we did not include ultimate failure and fracture in our constitutive model of the

tissue, the comparison between trabecular and cortical tissue material properties cannot be extended to ultimate properties.

Our results help resolve some of the controversy (Guo, 2001) on values of trabecular tissue elastic properties. Previous finite element studies on human vertebral (Hou et al., 1998; Ladd et al., 1998) and femoral (Ulrich et al., 1997) trabecular bone have reported notably low values of effective tissue moduli (Table 1). However, in a recent study (Niebur et al., 2000) and in this current study, finite element methods produced a much higher trabecular tissue effective modulus, comparable with that of cortical tissue. We believe the discrepancy between studies is mainly due to the presence of end-artifacts (Keaveny et al., 1997; Odgaard and Linde, 1991) in the earlier studies. Direct experimental measurements of trabecular tissue and cortical bone elastic properties have also resulted in contradicting conclusions (Guo, 2001). While some studies using nanoindentation have concluded that trabecular and cortical tissue elastic moduli are different (Rho et al., 1997; Zysset et al., 1999), one study using both acoustic microscopy and nanoindentation (Turner et al., 1999) concluded that they are similar. The low elastic modulus of trabecular tissue reported in the former studies (Rho et al., 1997; Zysset et al., 1999) is most likely due to the measurement of transverse modulus of the anisotropic tissue (Rho et al., 1997; Roy et al., 1996), and other factors such as spatial sampling and anatomic site-dependence may also have contributed. Interestingly, the cortical tissue moduli reported here are within 1% of previously reported values for human femoral cortical bone tissue measured using nanoindentation (Turner et al., 1999; Zysset et al., 1999). Given these uncertainties and the results presented here, we believe the weight of the evidence does support the concept that the effective tissue modulus of trabecular bone is at the higher end of the range of values reported in these nanoindentation studies (Table 1), and that the elastic modulus for trabecular tissue is only slightly lower than for cortical tissue.

Regarding strength properties, the available evidence is consistent in showing a lower strength for trabecular tissue, although the mechanisms remain unknown. Our finding that tissue strength is lower for trabecular tissue is consistent with results from fatigue studies on machined micro-beam specimens of trabecular and cortical tissue (Choi and Goldstein, 1992). In that study, our extrapolation of the reported fatigue $S-N$ curves to one cycle, which provides an estimate of the monotonic strength, shows that the tissue strength was about 15% lower for the trabecular bone. Further work is required to determine the microstructural sources of these differences, such as lamellar/collagen organization and orientation, mineralization, and failure modes (uniaxial vs. bending). Characterization of lamellar architecture and mineralization was beyond the scope of this study. Previous studies (Choi et al., 1990; Choi and Goldstein, 1992) have concluded that mineralization alone cannot explain differences in mechanical properties between the two types of tissue, but have raised the possibility of differences in lamellar architecture causing these differences. Another interesting avenue of research may be to explain the remarkably small inter-specimen variations observed in the yield strains of both trabecular and cortical tissue since providing such an explanation may reveal novel mechanisms by which bone has adapted to its function. All bone used in this study was "normal", and it would be interesting to determine if diseased bone displays altered tissue-level yield strain and strength-modulus relations.

Acknowledgements

This study was supported by grants from the National Institutes of Health (AR43784; AR41481), the National Science Foundation (BES-9625030), and the National Partnership for Advanced Computational Infrastructure (UCB254; UCB266). Cadaveric tissue was obtained from NDRI and UCSF Department of Anatomy. We would like to thank Dr. Sharmila Majumdar, Andrew Burghardt, Jacob Pollock, Margaretha Winata, Arul Krishnan, and Michael Y. Yu for their technical assistance.

References

Beck, J.D., Canfield, B.L., Haddock, S.M., Chen, T.J.H., Kothari, M., Keaveny, T.M., 1997. Three-dimensional imaging of trabecular bone using the computer numerically controlled milling technique. Bone 21, 281–287.

Burstein, A.H., Reilly, D.T., Martens, M., 1976. Aging of bone tissue: mechanical properties. Journal of Bone and Joint Surgery-American Volume 58, 82–86.

Choi, K., Goldstein, S.A., 1992. A comparison of the fatigue behavior of human trabecular and cortical bone tissue. Journal of Biomechanics 25, 1371–1381.

Choi, K., Kuhn, J.L., Ciarelli, M.J., Goldstein, S.A., 1990. The elastic moduli of human subchondral, trabecular, and cortical bone tissue and the size-dependency of cortical bone modulus. Journal of Biomechanics 23, 1103–1113.

Gibson, L.J., 1985. The mechanical behavior of cancellous bone. Journal of Biomechanics 18, 317–328.

Guldberg, R.E., Hollister, S.J., Charras, G.T., 1998. The accuracy of digital image-based finite element models. Journal of Biomechanical Engineering 120, 289–295.

Guo, X.E., 2001. Mechanical properties of cortical bone and cancellous tissue. In: Cowin, S.C. (Ed.), Bone Mechanics Handbook. CRC Press, Boca Raton, FL, pp. 10.11–10.23.

Heaney, R.P., 1993. Is there a role for bone quality in fragility fractures? Calcified Tissue International 53 (Suppl. 1), S3–6.

Hollister, S.J., Brennan, J.M., Kikuchi, N., 1994. A homogenization sampling procedure for calculating trabecular bone effective stiffness and tissue level stress. Journal of Biomechanics 27, 433–444.

Hou, F.J., Lang, S.M., Hoshaw, S.J., Reimann, D.A., Fyhrie, D.P., 1998. Human vertebral body apparent and hard tissue stiffness. Journal of Biomechanics 31, 1009–1015.

Hughes, T., Ferencz, R., Hallquist, J., 1987. Large-scale vectorized implicit calculation in solid mechanics on a cray x-mp/48 utilizing ebe preconditioned conjugate gradients. Computer Methods in Applied Mechanics and Engineering 61, 215–248.

Jaasma, M.J., Bayraktar, H.H., Niebur, G.L., Keaveny, T.M., 2002. Biomechanical effects of intraspecimen variations in tissue modulus for trabecular bone. Journal of Biomechanics 35, 237–246.

Jacobs, C.R., Davis, B.R., Rieger, C.J., Francis, J.J., Saad, M., Fyhrie, D.P., 1999. The impact of boundary conditions and mesh size on the accuracy of cancellous bone tissue modulus determination using large scale finite element modeling. Journal of Biomechanics 32, 1159–1164.

Keaveny, T.M., Wachtel, E.F., Ford, C.M., Hayes, W.C., 1994. Differences between the tensile and compressive strengths of bovine tibial trabecular bone depend on modulus. Journal of Biomechanics 27, 1137–1146.

Keaveny, T.M., Pinilla, T.P., Crawford, R.P., Kopperdahl, D.L., Lou, A., 1997. Systematic and random errors in compression testing of trabecular bone. Journal of Orthopaedic Research 15, 101–110.

Ladd, A.J., Kinney, J.H., Haupt, D.L., Goldstein, S.A., 1998. Finite-element modeling of trabecular bone: comparison with mechanical testing and determination of tissue modulus. Journal of Orthopaedic Research 16, 622–628.

Morgan, E.F., Keaveny, T.M., 2001. Dependence of yield strain of human trabecular bone on anatomic site. Journal of Biomechanics 34, 569–577.

Müller, R., Gerber, S.C., Hayes, W.C., 1998. Micro-compression: a novel technique for the nondestructive assessment of local bone failure. Technology and Health Care 6, 433–444.

Niebur, G.L., Yuen, J.C., Hsia, A.C., Keaveny, T.M., 1999. Convergence behavior of high-resolution finite element models of trabecular bone. Journal of Biomechanical Engineering 121, 629–635.

Niebur, G.L., Feldstein, M.J., Yuen, J.C., Chen, T.J., Keaveny, T.M., 2000. High-resolution finite element models with tissue strength asymmetry accurately predict failure of trabecular bone. Journal of Biomechanics 33, 1575–1583.

Odgaard, A., Linde, F., 1991. The underestimation of young's modulus in compressive testing of cancellous bone specimens. Journal of Biomechanics 24, 691–698.

Reilly, D.T., Burstein, A.H., 1975. The elastic and ultimate properties of compact bone tissue. Journal of Biomechanics 8, 393–405.

Rho, J.Y., Tsui, T.Y., Pharr, G.M., 1997. Elastic properties of human cortical and trabecular lamellar bone measured by nanoindentation. Biomaterials 18, 1325–1330.

Rho, J.Y., Roy, M.E., Tsui, T.Y., Pharr, G.M., 1999. Elastic properties of microstructural components of human bone tissue as measured by nanoindentation. Journal of Biomedical Materials Research 45, 48–54.

Roy, M., Rho, J.Y., Tsui, T.Y., Pharr, G.M., 1996. Variation of young's modulus and hardness in human lumbar vertebrae measured by nanoindentation. In: Proceedings of the Bioengineering Conference, Atlanta, GA, ASME BED 33, 385–386.

Silva, M.J., Gibson, L.J., 1997. Modeling the mechanical behavior of vertebral trabecular bone: effects of age-related changes in microstructure. Bone 21, 191–199.

Turner, C.H., Rho, J., Takano, Y., Tsui, T.Y., Pharr, G.M., 1999. The elastic properties of trabecular and cortical bone tissues are similar: results from two microscopic measurement techniques. Journal of Biomechanics 32, 437–441.

Ulrich, D., Hildebrand, T., van Rietbergen, B., Müller, R., Rüegsegger, P., 1997. The quality of trabecular bone evaluated with micro-computed tomography, fea and mechanical testing. Studies in Health Technology and Informatics 40, 97–112.

Ulrich, D., van Rietbergen, B., Weinans, H., Rüegsegger, P., 1998. Finite element analysis of trabecular bone structure: a comparison of image-based meshing techniques. Journal of Biomechanics 31, 1187–1192.

van der Linden, J.C., Birkenhager-Frenkel, D.H., Verhaar, J.A., Weinans, H., 2001. Trabecular bone's mechanical properties are affected by its non-uniform mineral distribution. Journal of Biomechanics 34, 1573–1580.

van Rietbergen, B., Weinans, H., Huiskes, R., Odgaard, A., 1995. A new method to determine trabecular bone elastic properties and loading using micromechanical finite element models. Journal of Biomechanics 28, 69–81.

Yeh, O.C., Keaveny, T.M., 1999. Biomechanical effects of intraspecimen variations in trabecular architecture: a three-dimensional finite element study. Bone 25, 223–228.

Zysset, P.K., Guo, X.E., Hoffler, C.E., Moore, K.E., Goldstein, S.A., 1999. Elastic modulus and hardness of cortical and trabecular bone lamellae measured by nanoindentation in the human femur. Journal of Biomechanics 32, 1005–1012.